

An 8-psec 13dBm Peak EIRP Digital-to-Impulse Radiator with an On-chip Slot Bow-Tie Antenna in Silicon

M. Mahdi Assefzadeh and Aydin Babakhani

Department of Electrical and Computer Engineering, Rice University, Houston, TX, 77005, USA

Abstract — In this paper, a direct digital-to-impulse transmitter is implemented that radiates impulses with EIRP of 13dBm and a record pulse-width of shorter than 8psec. It is shown that the starting time of the radiated impulses can be locked to the edge of the input trigger with a high timing accuracy. It is demonstrated that two widely spaced chips can generate coherent impulses in space with timing jitter of better than 270fsec. It is also shown that the frequency stability of the radiated impulses is better than 10Hz at 220GHz. The chip is fabricated in a 130nm SiGe BiCMOS process.

Index Terms — Coherent Spatial Combining, Picosecond Impulse Radiation, Direct Digital-to-Impulse Radiator, Slot Bow-Tie Antenna, SiGe, BiCMOS.

I. INTRODUCTION

There is a great interest in generating and radiating ultra-short pulses in mm-wave and THz regimes for applications in 3D imaging, spectroscopy, and high-speed wireless communication. Unfortunately, the pulse width of the prior silicon-based radiators is not short enough and their bandwidth is limited. In [1], a pulse-width of 45psec with bandwidth of 9.5% was achieved by modulating an on-chip continuous-wave (CW) source. The calculated 45psec was based on a frequency spectrum and no time-domain waveform was reported. In [2], the authors reported 26psec pulse-width with 33% bandwidth based on the noisy envelope of an RF signal that was not locked to the sampling oscilloscope. Due to the non-coherent method of the measurement, the actual time-domain waveform of the 26psec pulse was not observable. In [3], a frequency tunable radiating source with tuning range of 3% (10GHz at 280GHz center frequency) without pulse modulation capability was reported. The work in [1] and [3] offered no solution for locking the phase of the radiated signal to an external reference.

In contrast with the prior art [1-3], where a CW oscillator was modulated to generate ultra-short pulses, in this work, no oscillator is used. Instead, a direct digital-to-impulse converter and a broadband on-chip antenna are implemented that generate and radiate coherent impulses with a duration of 8psec, peak EIRP of 13dBm, and a repetition rate of more than 10GHz. These results are based on direct time-domain measurements using a sampling oscilloscope. In addition to the time-domain measurements, the frequency spectrum of impulse train is measured up to 220GHz. The radiated impulses can be locked to a digital trigger with timing jitter of better than 270fsec. This low level of the timing jitter, combined with the direct digital-to-impulse architecture of the circuit, makes it possible to build a coherent sparse array of

widely-spaced impulse-radiating chips with an effective aperture that is larger than the size of each individual antenna by several orders of magnitude. A large aperture is essential in generating images with high angular resolution. In order to demonstrate coherent spatial combining with widely-spaced elements, two impulse-radiating chips are placed with a spacing of 11 cm and their combined signal in the far-field is measured.

II. CIRCUIT ARCHITECTURE

The block diagram of the impulse radiator is shown in Fig. 1. A digital trigger signal with a rise time of 120psec is fed to the input of the chip. A series of digital buffers reduces the rise time of the signal to 30psec and sends it to a power amplifier (PA) for further amplification. A broadband slot bow-tie antenna is designed to radiate ultra-short impulses. The on-chip antenna is connected to a switch. When the switch is on, the antenna is energized by storing a DC current. When the switch is turned off by the PA, the current stored in the antenna radiates ultra-short impulses that are coherent with the digital trigger. Fig. 1 shows the schematic of the digital-to-impulse radiator. A transmission line based pulse matching network is used to maximize the energy of each impulse while minimizing its duration. As shown in Fig. 2, the pulse matching minimizes the ringing and duration of the impulse.

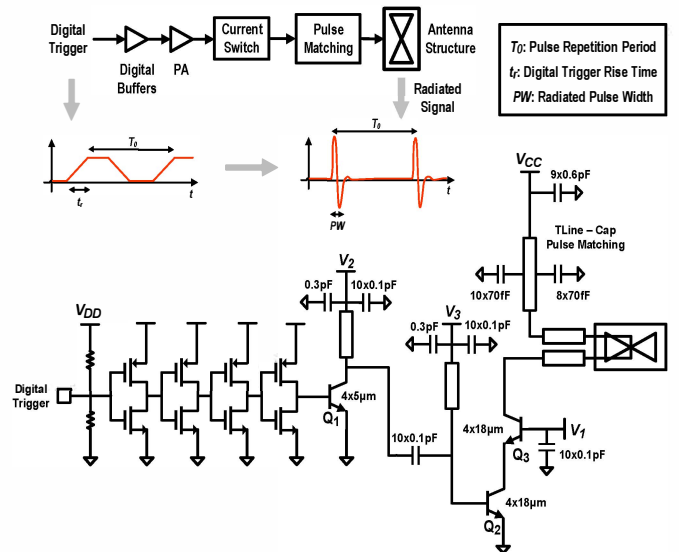


Fig. 1. Schematic of the digital-to-impulse radiator.

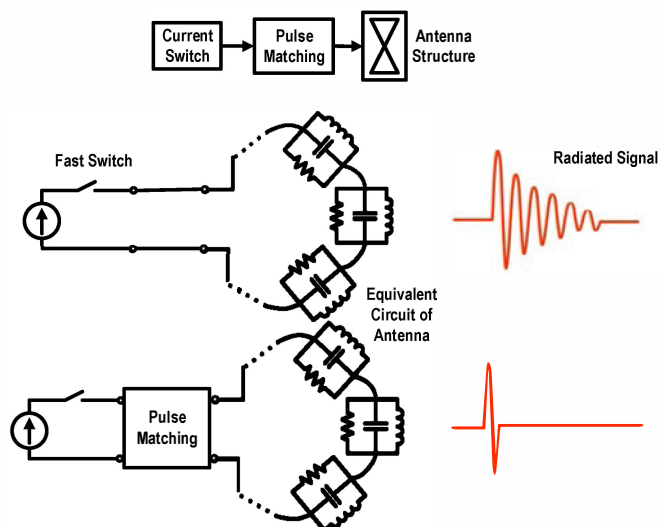


Fig. 2. Effect of the pulse matching network.

The impulse radiator can operate in two modes. In the first mode, a positive impulse is radiated that is locked to the rising edge of the input trigger. In the second mode, a negative impulse is radiated, which is locked to the falling edge of the input trigger. Depending on the biasing of node V_3 , only one or both of these modes can be activated. In addition, the amplitude of the radiated impulses can be modulated by the voltage at node V_2 , as shown in Fig. 1.

A distributed network of bypass capacitors is used at the biasing points to ensure fast delivery of electrical charges to the base node of transistor Q_3 . The edges of the slot bow-tie antenna are curved to improve its bandwidth. To minimize the substrate modes, increase the radiation efficiency, and minimize the ringing, the antenna is coupled to a silicon lens that has a radius of 6mm and an extension length of 0.4mm. The resistivity of the silicon lens is 10K Ω cm. The slot bow-tie antenna is implemented using a copper metal layer (M5). The matching transmission lines are fabricated using aluminum layers M6 and M7. The antenna is coupled to the silicon lens through the substrate.

III. MEASUREMENT RESULTS

One of the main challenges of measuring a time-domain waveform of a short impulse is the receiver of the measurement setup. The receiving antenna must have a constant group delay to prevent signal distortion. Although horn antennas were used in the prior art [2], due to the non-constant group delay of the horn antenna the received pulse becomes distorted. In this work, a custom impulse antenna with flat gain and constant group delay is used as the receiver. This receiving impulse antenna is fabricated on a printed circuit board (PCB) and has a dielectric constant of 2.4. Fig. 3 shows the fabricated antenna attached to a 1.85mm coaxial connector. Comparing the time domain signal received by the custom receiving antenna and the horn antenna confirmed that

horn antennas should not be used to measure ultra-short impulses. Therefore, we have only used horn antennas to extract the frequency spectrum of the impulse train. Fig. 4 shows the measured time-domain signal of the impulse-radiating chip (raw data), where the PCB-based custom antenna is used as the receiver. In this measurement, the receiving antenna is directly connected to an Agilent 86118A sampling head. A mm-wave lens with a focal point of 60mm is used to focus the power to the PCB antenna. In order to calculate the peak EIRP, the mm-wave lens is removed from the setup, and the loss of the cable/connector (~ 4 dB) is de-embedded. By using a center frequency of 50GHz in the Friis formula, a peak EIRP of 13dBm is calculated.

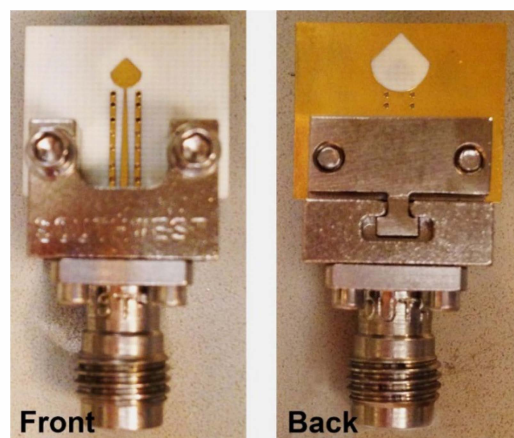


Fig. 3. Designed receiving impulse antenna with 1.85mm coaxial connector.

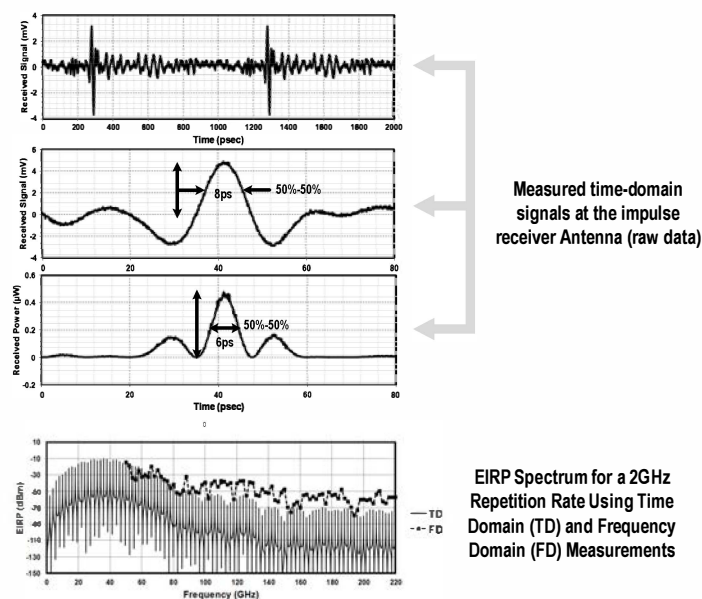


Fig. 4. Measured time-domain waveforms by the sampling oscilloscope. Spectrum of the EIRP calculated with both TD and FD measurements.

The time-domain radiation pattern of the impulse-radiating chip is measured. Fig. 5 shows the time-domain waveform as a function of angle in the E-plane of the antenna. In both E- and H- planes, it is confirmed that the waveform of the impulse is not distorted by changing the angle.

In addition to time-domain measurements, the frequency response of the impulse radiating chip is measured using an Agilent N9030A PXA Signal Analyzer, horn antennas, and OML harmonic mixers WR-15, WR-10, WR-08, and WR-05. The horn antennas and mixers cover the frequency range 50GHz to 220GHz. A distance of 370mm between the impulse radiating chip and the horn antenna is chosen. In this measurement no focusing lens is used. Fig. 4 shows the frequency-domain EIRP of the impulse radiator. In this measurement the loss of the mixer is de-embedded. The frequency spacing between the points in this diagram is equal to the repetition rate of 2GHz. The radiation pattern of the impulse radiating chip at 70GHz is reported in Fig. 5.

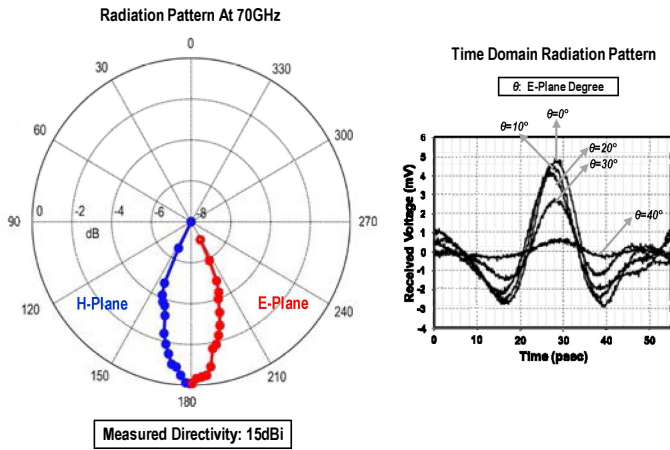


Fig. 5. Radiation pattern of the impulse radiator in FD (left) and TD (right) measurements.

IV. COHERENT COMBINING OF IMPULSES IN SPACE

The precision synchronization of the digital trigger with the radiated impulses makes it possible to build a coherent sparse array with widely-spaced antennas to increase the effective aperture size. To demonstrate a coherent array, the radiated impulses from two separate chips are combined in the far-field. The digital trigger signal of each chip is provided by Tektronix Arbitrary Waveform Generator AWG7000. The AWG generates two synchronized trigger signals that can be shifted with respect to each other with a resolution of 1ps. Fig. 6 shows the time-domain waveform of two impulse radiating chips and their combined signal.

The timing jitter of the combined signal is calculated by an Agilent sampling oscilloscope 86100DCA as shown in Fig. 7. An RMS jitter of 270fs is measured with an averaging of 64. Averaging is used to reduce the noise of the Agilent 86118A sampling head. The measured RMS jitter for averaging of 256

and 512 is 220fs and 130fs, respectively. One of the unique features of the coherent impulse-radiating chip is the high spectral purity of the radiated impulses. Based on the measured spectrum, 99% of the power of the 220GHz tone is concentrated between frequencies 220,000,022,180Hz and 220,000,022,190Hz, which is only 10Hz (Fig. 7). This level of frequency stability is essential in performing high-resolution frequency-domain spectroscopy.

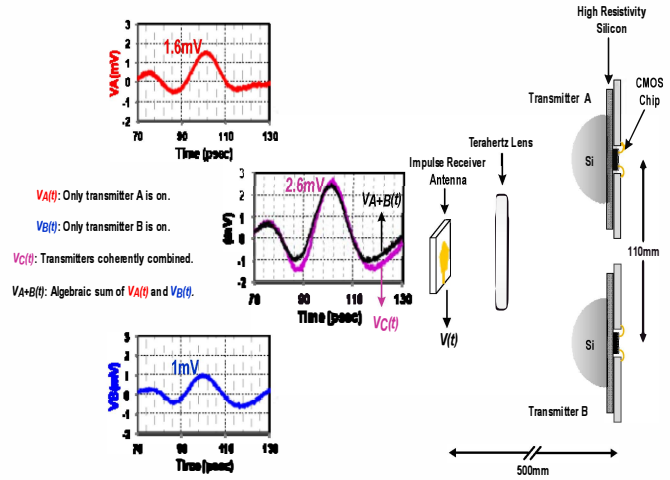


Fig. 6. Coherent combining of widely spaced impulse radiating chips, set-up, and measurement results.

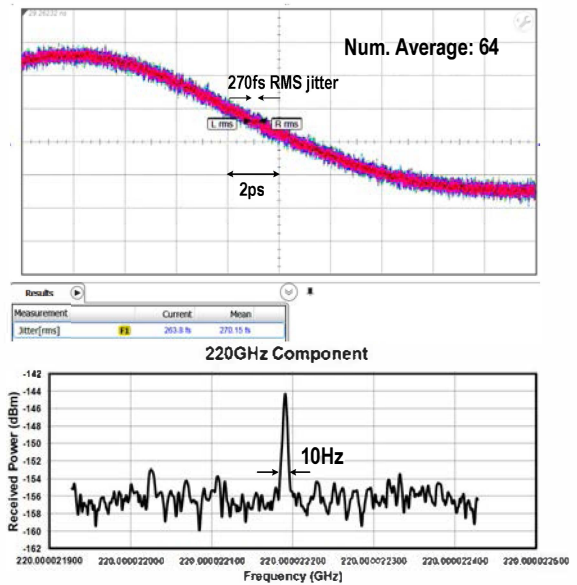


Fig. 7. Jitter of the coherently combined signal, and the un-calibrated power spectrum around 220GHz. 99% of the 220GHz tone is confined in less than 10Hz frequency range.

To the best of the Authors' knowledge, this is the first coherent impulse-radiating array with widely spaced antennas that can radiate sub-8 psec impulses.

Table I compares the specifications of the reported chip with the prior art. The reported digital-to-impulse radiating

TABLE I
COMPARISON TABLE

	This work	[1] ISSCC 2013	[2] JSSC 2013	[3] JSSC 2012
Shortest Radiated Pulse (psec)	8 (50%-50%)	45	26 (50%-50%)	CW only
Peak EIRP (dBm)	13	15.7	13	9.4
Phase Synchronization with an External Reference	Yes	No	Yes	No
Coherent Spatial Combining with Multiple Chips	Performed	N/A	N/A	N/A
Time-domain Measurements	Yes (with locking)	N/A	Yes (without locking)	N/A
Frequency-domain Measurements	Yes	Yes	Yes	Yes
Pulse Generation Method	Digital-to-Impulse	Oscillator-based	Oscillator-based	Oscillator-based
Power Consumption (mW)	220	800	580	820
Technology	0.13 μ m SiGe BiCMOS	65nm CMOS	0.13 μ m SiGe BiCMOS	45nm SOI CMOS
Die Area (mm ²)	0.47	2.25	6.16	7.29

chip was fabricated in a 130nm SiGe BiCMOS process technology with $f_T = 200\text{GHz}$ and $f_{max} = 270\text{GHz}$. A micrograph of the chip is shown in Fig. 8. The size of the chip, including the on-chip antenna and the pads, is $0.55\text{mm} \times 0.85\text{mm}$.

- [3] K. Sengupta, and A. Hajimiri, "A 0.28 THz Power-Generation and Beam-Steering Array in CMOS Based on Distributed Active Radiators," *Solid-State Circuits, IEEE Journal of*, vol.47, no.12, pp.3013,3031, Dec. 2012.

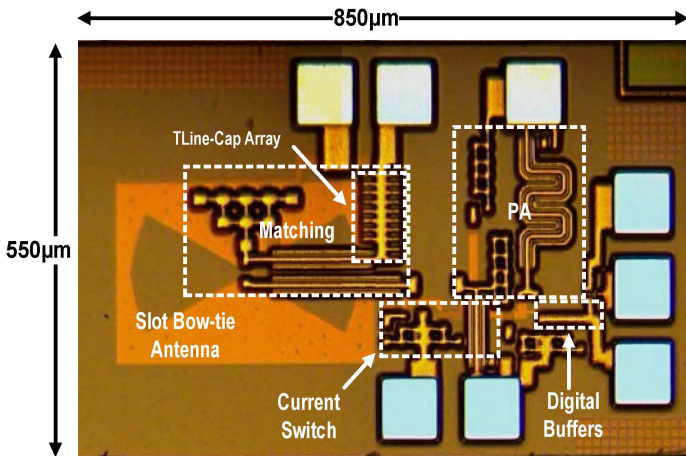


Fig. 8. Micrograph of the chip.

ACKNOWLEDGEMENT

This work was supported by DARPA MTO office under YFA and LEAP programs. Authors appreciate the support of Dr. William Chappell.

REFERENCES

- [1] R. Han, and E. Afshari, "A 260GHz broadband source with 1.1mW continuous-wave radiated power and EIRP of 15.7dBm in 65nm CMOS," *Solid-State Circuits Conference Digest of Technical Papers (ISSCC), 2013 IEEE International*, vol., no., pp.138,139, 17-21 Feb. 2013.
- [2] A. Arbabian, S. Callender, S. Kang, M. Rangwala, and A.M. Niknejad, "A 94 GHz mm-Wave-to-Baseband Pulsed-Radar Transceiver with Applications in Imaging and Gesture Recognition," *Solid-State Circuits, IEEE Journal of*, vol.48, no.4, pp.1055,1071, April 2013.